

Learning Compact Boolean Networks

Shengpu Wang¹ Yuhao Mao² Yani Zhang¹ Martin Vechev²

Abstract

Floating-point neural networks dominate modern machine learning but incur substantial inference cost, motivating interest in Boolean networks for resource-constrained settings. However, learning compact and accurate Boolean networks is challenging due to their combinatorial nature. In this work, we address this challenge from three different angles: learned connections, compact convolutions and adaptive discretization. First, we propose a novel strategy to learn efficient connections with no additional parameters and negligible computational overhead. Second, we introduce a novel convolutional Boolean architecture that exploits the locality with reduced number of Boolean operations than existing methods. Third, we propose an adaptive discretization strategy to reduce the accuracy drop when converting a continuous-valued network into a Boolean one. Extensive results on standard vision benchmarks demonstrate that the Pareto front of accuracy vs. computation of our method significantly outperforms prior state-of-the-art, achieving better accuracy with up to 37x fewer Boolean operations.

1. Introduction

Despite the success of neural networks in various domains, their high inference cost causes heavy burden on the environment and limits their deployment in resource-constrained environments such as edge devices and IoT applications. A promising solution is to learn Boolean networks (a special family of Boolean circuits, c.f. §3) that operate directly on Boolean values, i.e., 0 and 1, instead of on floating-point numbers, because Boolean operations are inherently more efficient in terms of computation, memory

¹Department of Information Technology and Electrical Engineering, ETH Zurich ²Department of Computer Science, ETH Zurich. Correspondence to: Shengpu Wang <wangshen@ethz.ch>, Yuhao Mao <yuhao.mao@inf.ethz.ch>, Yani Zhang <yanizhang@mins.ee.ethz.ch>, Martin Vechev <martin.vechev@inf.ethz.ch>.

Preprint. February 6, 2026.

and power consumption.

A smaller Boolean circuit is generally cheaper to execute. For a given Boolean function, finding a compact, or even minimal, Boolean circuit implementing this function is a fundamental and well-studied problem (Rudell & Sangiovanni-Vincentelli, 1987; Ganai & Kuehlmann, 2000; Micheli, 1994; Bjesse & Boralv, 2004; Mishchenko et al., 2006a; Riener et al., 2022). However, in practice, the Boolean function is often not known a priori and must be learned from data.

This Work: Learning Compact and Accurate Boolean Networks Efficiently We build on the learning framework proposed by Petersen et al. (2022). It works by first relaxing a Boolean network into a differentiable representation and training it with gradient-based methods, and then discretizing it back into a Boolean network. Despite existing efforts, three key challenges remain open. (i) *Efficient connection learning*. Petersen et al. (2022; 2024) and Rüttgers et al. (2025) randomly sample fixed connections between layers. However, according to the lottery ticket hypothesis (Frankle & Carbin, 2019), the ultra sparsity of Boolean networks (two inputs per neuron) makes random choices highly ineffective. On the other hand, Baccellar et al. (2024) and Fojcik et al. (2025) parameterize the network connection with additional weight matrices, but this leads to significant memory and computational overhead during training, typically quadratic in the number of neurons per layer. (ii) *Compact convolutional architecture*. The existing convolutional Boolean architecture (Petersen et al., 2024) utilizes a hardcoded tree-like kernel, which requires more Boolean operations (exponential in the depth of the tree) than a non-convolutional layer. (iii) *Discretization-aware training*. The discrepancy between the differentiable relaxation and the discrete Boolean network causes a clear accuracy drop after discretization.

In this paper, we address the aforementioned challenges and propose a novel method for learning compact Boolean networks. Our contributions are summarized as follows.

Main Contributions

- We introduce a novel strategy to learn efficient connectivity for Boolean networks with no additional pa-

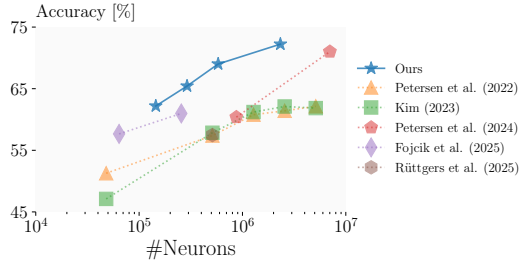


Figure 1. Comparison between our method and prior works on CIFAR-10. Note the log scale on x-axis.

rameters and negligible computational overhead.

- We propose a compact convolutional Boolean architecture, removing hardcoded tree structures and reducing the number of Boolean operations.
- We develop an adaptive discretization strategy that progressively discretizes network layers during training, effectively reducing the discretization gap and improving final performance.
- Through extensive evaluation on vision benchmarks, we demonstrate that our method consistently learns more compact Boolean networks with higher accuracy (Fig. 1), achieving up to 37x fewer Boolean operations with better accuracy on MNIST when compared to Petersen et al. (2024), the prior state-of-the-art.

The rest of the paper is organized as follows. §2 reviews the literature on learning Boolean structures and reducing the inference cost of floating-point neural networks. §3 introduces the necessary background on learning Boolean networks via differentiable relaxations. §4 and §5 presents and extensively evaluates our method, respectively. Finally, §6 discusses the limitations and potential future directions.

2. Related Work

Improving Inference Efficiency Many works aim to reduce the inference cost of neural networks, typically via quantization and pruning. Quantization reduces operation costs by lowering the precision of weights, while pruning removes partial connections from the network to reduce the number of operations. We refer to Gholami et al. (2021) and Liu et al. (2025) for a comprehensive survey on quantization, and to Cheng et al. (2024) for a comprehensive survey on pruning. These methods motivate the study of Boolean networks, which replace floating-point operations with Boolean operations, significantly reducing operation cost and connection density simultaneously.

Learning Boolean Structures We review prior works on learning three different Boolean structures: Boolean networks, binary decision diagrams (BDDs), and lookup-tables (LUTs). Petersen et al. (2022) first proposed differentiable learning of Boolean networks. Many later works

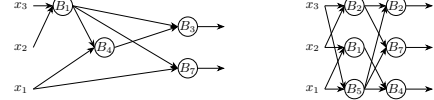


Figure 2. Left: a Boolean circuit. Right: a Boolean network.

improved the learning of Boolean networks: Rüttgers et al. (2025) reduced the parameter overhead during training; Baccellar et al. (2024) and Fojcik et al. (2025) introduced learnable connections between layers; Petersen et al. (2024) designed convolutional Boolean networks; Bührer et al. (2025) extended Boolean networks to recurrent architectures. For BDDs, Shati et al. (2023) and Florio & Martins (2023) formulated BDD learning as a SAT problem; Zantedeschi et al. (2021) trained discrete decision trees via argmin differentiation; Qiu et al. (2025) proposed to parameterize ordered BDDs with continuous encodings, and then read off discrete BDDs after training. For LUTs, Umuroglu et al. (2020) reduced sparse quantized networks into LUT networks; Wang et al. (2019) trained LUT networks via Lagrange-interpolating polynomial relaxations; Andronic & Constantinides (2025) proposed a hardware-aware training and assembly strategy for LUT networks; Cassidy et al. (2025) performed post-training LUT compression; Weng et al. (2025) assembles multiple small LUT subnetworks to form a larger LUT network.

3. Background

Boolean Circuits and Boolean Networks Boolean circuits are directed acyclic graphs where each node computes a bivariate Boolean function $B : \{0, 1\}^2 \rightarrow \{0, 1\}$ (Arora & Barak, 2009). We denote the 16 possible bivariate Boolean functions by $\mathbb{B} := \{B_i : \{0, 1\}^2 \rightarrow \{0, 1\}, i = 1, \dots, 16\}$ (c.f. §1). A Boolean network is a Boolean circuit where nodes and edges are arranged in layers. Fig. 2 illustrates a Boolean circuit and a Boolean network.

Boolean circuits realize only Boolean functions. To apply them to implement a non-Boolean function $g : A \rightarrow B$, we need to decompose g into a Boolean function $f : \{0, 1\}^m \rightarrow \{0, 1\}^n$, $m, n \in \mathbb{N}$, together with an encoder $\mathcal{E} : A \rightarrow \{0, 1\}^m$ and a decoder $\mathcal{D} : \{0, 1\}^n \rightarrow B$, such that $g = \mathcal{D} \circ f \circ \mathcal{E}$. In particular, for an image classification function $g : [0, 1]^d \rightarrow \mathcal{C}$ that takes a real-valued image and maps it to a class label, we use the thermometer encoder, defined as $\mathcal{E}(\mathbf{x}) := [\mathbb{1}\{\mathbf{x} \geq \frac{1}{N}\}, \dots, \mathbb{1}\{\mathbf{x} \geq \frac{N-1}{N}\}]$, where $\mathbb{1}\{\cdot\}$ is the indicator function. We use the population count decoder (also named GroupSum) selecting the class with the highest number of 1s in the output Boolean vector $\mathbf{Y} \in \{0, 1\}^{|\mathcal{C}| \times n_c}$, defined as $\mathcal{D}(\mathbf{Y}) := \arg \max_{c \in \mathcal{C}} \sum_{i=1}^{n_c} \mathbf{Y}_{c,i}$.

Learning Boolean Networks via Differentiable Relaxations To learn a Boolean network from data, Petersen

et al. (2022) propose to relax discrete Boolean networks into differentiable functions, enabling training via gradient descent. Specifically, for $i = 1, \dots, 16$, let $B_i^c : [0, 1]^2 \rightarrow [0, 1]$ be a differentiable relaxation of B_i . For example, $B_2(x_b, y_b) = x_b \wedge y_b, x_b, y_b \in \{0, 1\}$, is relaxed into $B_2^c(x, y) = xy, x, y \in [0, 1]$, satisfying $B_2^c(x_b, y_b) = B_2(x_b, y_b)$. Each neuron is then parametrized as a weighted aggregation of all B_i^c as

$$f^c(x, y) = \sum_{i=1}^{16} \frac{\exp(\mathbf{w}_i)}{\sum_{j=1}^{16} \exp(\mathbf{w}_j)} B_i^c(x, y), \quad (1)$$

where \mathbf{w}_i are the parameters. Afterwards, the relaxed network is trained on data by updating the weight vector $\mathbf{w} = (\mathbf{w}_1, \dots, \mathbf{w}_{16})$ of each neuron. Finally, each neuron is discretized back to a bivariate Boolean function by

$$f := B_{i^*}, \quad \text{with } i^* = \arg \max_i \mathbf{w}_i. \quad (2)$$

Note that the relaxation and parametrization above only allows to learn the Boolean operation at each neuron, but does not allow the learning of network connections. We shall address the efficient connection learning later in §4.

Convolutional Boolean Networks Convolutional layers are key components in floating-point neural networks capturing local spatial structures. Petersen et al. (2024) design a convolutional architecture for Boolean networks, where each kernel is a binary tree consisting of Boolean operations. A tree of depth d requires $2^d - 1$ Boolean operations to implement a Boolean function with 2^{d-1} inputs. As a result, their convolutional layer costs significantly more Boolean operations than a non-convolutional layer.

4. Learning Compact Boolean Networks

In this section, we introduce our methods to learn compact and accurate Boolean networks. We first present an efficient connection learning strategy in §4.1, which is based on a novel parameterization of Boolean neurons that aggregates information from multiple connections, and an adaptive resampling strategy to continuously explore new connections. Next, we present a compact convolutional Boolean architecture in §4.2, replacing tree structures with single-operation kernels enabled by connection learning. Finally, we introduce an adaptive discretization strategy in §4.3, progressively discretizing network layers during training to reduce the accuracy drop.

4.1. Efficient Connection Learning

We modify the parameterization in Equation (1) to allow connection learning as follows. Instead of parameterizing neurons as a weighted aggregation of sixteen Boolean operations with the same inputs, we assign different inputs to

different Boolean operations. Specifically, let $\mathbf{x} \in [0, 1]^d$ be the vector representing the d neurons in the ℓ -th layer. For a neuron in the $(\ell + 1)$ -th layer, we parameterize it as

$$\tilde{f}^c(\mathbf{x}; \mathbf{k}, \mathbf{p}, \mathbf{q}) = \sum_{i=1}^{16} \frac{\exp(\mathbf{w}_i)}{\sum_{j=1}^{16} \exp(\mathbf{w}_j)} B_{\mathbf{k}_i}^c(\mathbf{x}_{\mathbf{p}_i}, \mathbf{x}_{\mathbf{q}_i}), \quad (3)$$

where $\mathbf{k} \in \{1, \dots, 16\}^{16}$ are indices denoting the Boolean operations, and $\mathbf{p}, \mathbf{q} \in \{1, \dots, d\}^{16}$ are indices denoting the two input neurons from the ℓ -th layer, respectively. At the beginning of training, $(\mathbf{k}, \mathbf{p}, \mathbf{q})$ can be sampled uniformly at random or follow any specific assignments. See Fig. 3 for an illustration of the parameterization.

For each neuron, the optimal combination of inputs and Boolean function might not be included in the initial assignment. To learn better combinations, we propose an adaptive resampling strategy. The high-level idea is: once a neuron becomes “stable” during training, we resample its $(\mathbf{k}, \mathbf{p}, \mathbf{q})$ candidates to explore new combinations. We measure the stability of a neuron by monitoring its weight entropy, defined as:

$$h(\mathbf{w}) = - \sum_{i=1}^{16} \tilde{w}_i \log \tilde{w}_i, \quad \text{where } \tilde{w}_i = \frac{\exp(\mathbf{w}_i)}{\sum_{j=1}^{16} \exp(\mathbf{w}_j)}.$$

The weight entropy equals zero if and only if one element in the normalized weight $\tilde{\mathbf{w}}$ equals one, indicating that the neuron is represented by a single $(\mathbf{k}_i, \mathbf{p}_i, \mathbf{q}_i)$ triple, and reaches its maximum when all elements in $\tilde{\mathbf{w}}$ are equal, indicating that the neuron is an equal mixture of all $(\mathbf{k}_i, \mathbf{p}_i, \mathbf{q}_i)$ triples. We track the exponential moving average (EMA) of the weight entropy for each neuron individually. When the EMA of $h(\mathbf{w})$ for a neuron converges, its weight vector \mathbf{w} can have three possible states: (i) dominated by a single triple $(\mathbf{k}_i, \mathbf{p}_i, \mathbf{q}_i)$, i.e., $\exists i^*, \tilde{w}_{i^*} \geq 0.95$; (ii) dispersed, i.e., $\max_i \mathbf{w}_i \leq 0.4$; (iii) concentrated without a dominant triple. For (i), further training of the neuron is unlikely to improve the discretized network unless the dominant triple is replaced, so we resample all $(\mathbf{k}_i, \mathbf{p}_i, \mathbf{q}_i)$ except the dominant one to explore new combinations. For (ii), the neuron fails to find a useful triple, thus we resample all $(\mathbf{k}_i, \mathbf{p}_i, \mathbf{q}_i)$ to restart its learning. Neurons falling into the third case are not changed since they are still learning. We refer to the pseudocode in Algorithm 1 for further details. We note that after training, most neurons (frequently over 90%) empirically end up in the first case, indicating that they have learned meaningful patterns expressed by a single dominant connection and Boolean function.

We remark on the relation to prior works and the overhead of the proposed method. As mentioned in §1, Petersen et al. (2022; 2024) and Rüttgers et al. (2025) randomly sample the connection and keep it fixed during training. To allow learning connections, Bacellar et al. (2024) and Fojcik

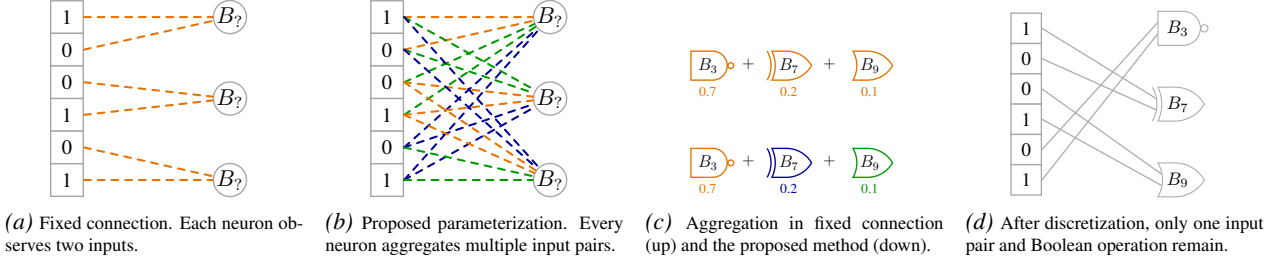


Figure 3. Comparison between the parameterization with fixed connections (literature) and the proposed parameterization.

Algorithm 1 Adaptive Resampling

Input: initial neuron weight $w \in \mathbb{R}^{16}$, weight update function STEP, EMA momentum ρ , stability threshold ϵ , patience T , #triples per neuron $K = 16$.

Output: trained neuron weight w

```

 $\mu \leftarrow 0, c \leftarrow 0$ 
repeat
     $w \leftarrow \text{STEP}(w)$ 
     $h \leftarrow -\sum_{i=1}^K \tilde{w}_i \log \tilde{w}_i$ , where  $\tilde{w}_i = \frac{\exp(w_i)}{\sum_j \exp(w_j)}$ 
    Increase  $c$  by 1 if  $|\mu - h| \leq \epsilon$ , else set  $c \leftarrow 0$ 
     $\mu \leftarrow \rho\mu + (1 - \rho)h$ 
    if  $c \geq T$  then
        dominated  $\leftarrow$  check if  $\exists i^*, \tilde{w}_{i^*} \geq 0.95$ 
        dispersed  $\leftarrow$  check if  $\max_i \tilde{w}_i \leq 0.4$ 
        if dominated then
            resample all  $(k_i, p_i, q_i)$  except the dominant one
            reset  $w$  such that  $\tilde{w}_{i^*} = 0.9$  and  $\tilde{w}_j = \frac{0.1}{K-1}$  for  $j \neq i^*$ 
        else if dispersed then
            resample all  $(k_i, p_i, q_i)$ 
            reset  $w$  such that  $\tilde{w}_i = \frac{1}{K}$  for all  $i$ 
        end if
    end if
    reset  $c \leftarrow 0$  if resampling is performed
until training ends
    
```

et al. (2025) propose to parameterize the connections with additional weight matrices. A Boolean layer with d_{in} input neurons and d_{out} output neurons additionally maintains a weight matrix $W_{\text{link}} \in \mathbb{R}^{d_{in} \times d_{out}}$. However, such large matrices are often impractical: for a typical medium-sized model in Petersen et al. (2024), W_{link} for a single layer can consume over 3400 GB of memory. In contrast, our method learns the network connection without additional parameters. Nevertheless, compared to Petersen et al. (2022; 2024), it does introduce mild computational and memory overhead during training (but not at inference): EMAs are tracked (a scalar per neuron), and resampling is performed periodically. However, these overheads are typically negligible compared to the overall training cost.

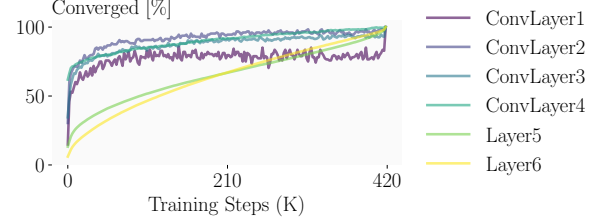


Figure 4. Convergence speed of different layers.

4.2. Convolution without Boolean Trees

Convolution is a key component in floating-point neural networks to capture spatial features, especially for vision tasks. A natural and easy way to construct convolutional layers in Boolean networks is to take a single Boolean operation as the convolutional kernel. However, such kernels under fixed connections only observe two inputs from the receptive field. With the design in §4.1, this does not constitute a problem: a convolutional kernel learns to extract important information from the full receptive field by aggregating multiple input pairs during training, thus the kernel can observe up to 32 distinct inputs from the receptive field. As a result, we can learn a compact convolutional Boolean network based on single-operation kernels.

In contrast, the convolutional kernels in Petersen et al. (2024) are built on Boolean trees. Specifically, 2^{d-1} neurons sampled from the receptive field are fed into a binary Boolean tree of depth d , and then every node in the tree is learned with the relaxation in Equation (1). Such tree structure has two main issues. First, the number of Boolean operations per layer grows exponentially with the tree depth d , leading to high inference costs. Second, the hierarchical structure of binary trees introduces sequential dependencies that limit parallelism during both forward and backward passes. As we later demonstrate empirically in §5, our method can learn much smaller convolutional Boolean networks with higher accuracies.

4.3. Adaptive Discretization

As introduced in §3, after training, the network is discretized to Boolean by replacing all relaxed neurons with

their dominant Boolean operation at once. However, such training paradigm ignores the discrepancy between the continuous and Boolean networks, and thus leads to a systematic accuracy drop after discretization. We shall address the discretization issue in this subsection.

During training, convolutional layers of the network tend to converge faster than the non-convolutional layers. We measure the ratio of neurons that have the same dominant (k_i, p_i, q_i) triple as the final discretized network. As shown in Fig. 4, convolutional layers converge much faster than non-convolutional layers. Further, convolutional layers tend to be less stable, e.g., the first convolutional layer stops improving when roughly 80% neurons converge, while non-convolutional layers converge more steadily. Based on these observations, we propose to adaptively discretize (and thus freeze) the network progressively from shallow to deep layers during training. Specifically, we monitor the convergence of each layer using the average weight entropy and EMAs, similar to §4.1. Once the first layer converges, we immediately discretize it by Equation (2) (thus stop training it) and continue training the subsequent layers. We proceed layer-wise in this manner for all convolutional layers, and then continue training the non-convolutional layers in their relaxed form until the end. A pseudocode is provided as Algorithm 2. The progressive discretization forces the layers to adapt to Boolean inputs during training. As a result, the network suffers less from the accuracy drop caused by discretization.

We remark that Kim (2023) and Yousefi et al. (2025) attempt to mitigate the discretization issue as well, but via injecting noise during training. However, the injected noise distribution does not accurately reflect the true distribution of the discretization error, and thus fails to guide the training towards better solutions (c.f. §5.3).

5. Experiments

In this section, we empirically evaluate the proposed methods on image classification tasks, both separately and in combination. We first describe the experimental setup, including the data augmentation, input encoding and output decoding schemes. The metrics and baselines are then detailed. We present results on learned connections (§5.1), the convolutional architecture (§5.2), and the adaptive discretization strategy (§5.3), building up to the final combined results (§5.4).

Setup We evaluate our method on MNIST (LeCun et al., 1998) and CIFAR-10 (Krizhevsky et al., 2009). For MNIST, we round the floating-point pixels to the closest Boolean values, and apply random rotations (up to 15°) and random affine transformations (with translations up to 10% of the image size in both spatial directions) as data

Algorithm 2 Adaptive Discretization

Input: weights \mathbf{W} returned by Algorithm 1, weight update function STEP, EMA momentum ρ , stability threshold ϵ , patience T .
Output: discretized Boolean network
repeat
 $\mathbf{W} \leftarrow \text{STEP}(\mathbf{W})$
 $l \leftarrow$ the first non-discretized layer
 Initialize $\mu_l \leftarrow 0$, $c_l \leftarrow 0$ if not initialized
 Compute average weight entropy h_l
 Increase c_l by 1 if $|\mu_l - h_l| \leq \epsilon$, else set $c_l \leftarrow 0$
 $\mu_l \leftarrow \rho\mu_l + (1 - \rho)h_l$
 if $c_l \geq T$ **then**
 Freeze and discretize layer l using Equation (2)
 Mark layer l as discretized
 end if
until training ends

augmentation during training. On CIFAR-10, we use thermometer encoding with equal thresholds (c.f. §3) to convert floating-point pixels to Boolean strings with various lengths, following Petersen et al. (2022; 2024); for convolutional networks, we concatenate these Boolean strings along the channel dimension. Random horizontal flips and random crops of size 32×32 with a padding of 2 pixels are applied during training. No data augmentation is applied at inference on both datasets. The population count decoder as described in §3 is applied on both datasets. Further experimental details are included in §F.

Metrics We use test accuracy as the performance metric. To measure the Boolean circuit size, we use two metrics: the number of neurons in the Boolean network (#neurons), and the number of Boolean operations in the pruned Boolean circuit (#BOPs). The pruning simply removes all redundant neurons that have no contribution to the final output, and removes Identity and NOT neurons by rewiring their input connections to their output connections (see §E for details). We note that more advanced logic synthesis methods (Mishchenko et al., 2006b; Brayton & Mishchenko, 2010; Riener et al., 2019; Li et al., 2024) can be applied to further reduce the circuit size after pruning; we apply the simplest pruning to avoid bias towards any specific circuit optimization method. We remark that since all baselines and our method are not trained with circuit optimization in the loop, the relative comparisons before and after pruning (i.e., #neurons and #BOPs) are similar for our empirical studies. Therefore, we expect the relative performance gain of our method over baselines to hold as well after applying more advanced logic synthesis techniques.

Baselines For the connection learning and convolution design, we compare against DiffLogicNet (Petersen et al.,

Table 1. Comparison between DiffLogicNet and our method on MNIST.

Method	Acc.	#neurons	#BOPs
DiffLogicNet (small)	97.16%	48.0 K	26.9 K
DiffLogicNet (medium)	98.80%	384 K	214 K
Ours (small)	97.95%	48.0 K	25.0 K
Ours (medium)	99.10%	384 K	190 K

Table 2. Comparison between DiffLogicNet and our method on CIFAR-10.

Method	Acc.	#neurons	#BOPs
DiffLogicNet (small)	52.84%	48.0 K	27.0 K
DiffLogicNet (medium)	59.90%	512 K	312 K
DiffLogicNet (large)	62.57%	1.28 M	780 K
Ours (small)	56.13%	48.0 K	27.0 K
Ours (medium)	62.84%	512 K	297 K
Ours (large)	64.53%	1.28 M	705 K

2022) and TreeLogicNet (Petersen et al., 2024), respectively. We take the official implementation for DiffLogicNet, and the community implementation that matches the results reported in Petersen et al. (2024) for TreeLogicNet (see §C for details) since the official implementation is not publicly available. For the adaptive discretization, we compare against Gumbel noise injection (Yousefi et al., 2025) with the official implementation. We apply the same input encoding, output decoding, data augmentation, and model optimizer across all methods for fair comparison.

5.1. Connection Learning

We focus on evaluating the effectiveness of the proposed connection learning method in §4.1. Specifically, we compare our models against DiffLogicNet, under strictly identical conditions, including network architecture (except the parameterization) and data processing.

Main Results The results on MNIST and CIFAR-10 are summarized in Table 1 and Table 2, respectively. Across all datasets and model sizes, learned connections consistently outperform DiffLogicNet which uses fixed connections. Notably, on CIFAR-10, our method uses only 512K neurons to achieve better accuracy than DiffLogicNet with twice the number of neurons (1.28M). On average, models with our connection learning achieve 0.55% and 2.73% higher accuracy on MNIST and CIFAR-10, respectively.

The More Learned, the Better Bacellar et al. (2024) reported that for their proposed connection learning algorithm, only learning the connections in the first layer can achieve performance comparable to fully learnable models, suggesting inefficiency in learning connections in deeper layers. To verify the effectiveness of our method in learning connections across all layers, we conduct an ablation study

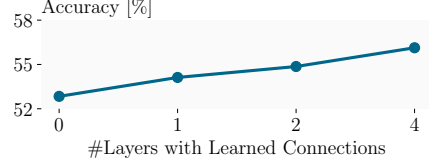


Figure 5. The result of learning partial connections on CIFAR-10. Note that the x-axis is unequally spaced.

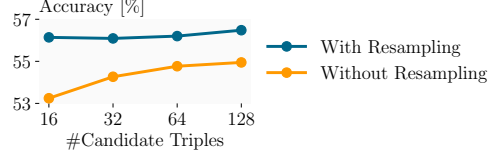


Figure 6. The effect of increasing the number of candidate triples, with and without resampling. Note the log scale on x-axis.

on CIFAR-10 with the small model, varying the number of layers with learned connections. Layers beyond the learned ones use fixed random connections as in DiffLogicNet. As shown in Fig. 5, learning connections in more layers with our proposed method consistently improves the accuracy, demonstrating the effectiveness of our method in learning connections both in shallow and deep layers.

Resampling vs More Candidates As discussed in §4.1, resampling aims to explore new candidates during training. One direct alternative is to simply increase the number of candidate triples (k_i, p_i, q_i) per neuron, from 16 to a larger number K . Such choices naturally allows the neuron to aggregate information from a larger pool of candidates. However, we shall show that with the proposed resampling strategy, increasing the number of candidates is unnecessary, thereby saving computation and memory during training. To verify this, we conduct an ablation study on CIFAR-10 with the same small model, varying the number of candidates K from 16 to 128. As shown in Fig. 6, without resampling, increasing K from 16 to 128 improves the accuracy clearly, from 53.24% to 54.94%. However, with resampling, the accuracy gain becomes marginal, from 56.14% to 56.48%. Further, for all K , resampling consistently outperforms the non-resampling counterpart. These results validate the effectiveness of the proposed resampling strategy in exploring new candidates during training, thus removes the necessity of introducing more candidates and the associated memory and computational overhead.

5.2. Convolution

In this part, we evaluate the proposed convolutional architecture that uses a single Boolean operation for the convolutional kernel, against TreeLogicNet that uses Boolean trees for convolutional kernels. Both architectures use 3x3 re-

Table 3. Comparison between TreeLogicNet and our method on MNIST.

Method	Acc.	#neurons	#BOPs
TreeLogicNet-S	97.81%	185 K	117 K
TreeLogicNet-M	98.95%	740 K	427 K
TreeLogicNet-L	99.32%	11.8 M	6.20 M
Ours-S	99.12%	260 K	165 K
Ours-M	99.35%	520 K	240 K

Table 4. Comparison between TreeLogicNet and our method on CIFAR-10.

Method	Acc.	#neurons	#BOPs
TreeLogicNet-S	59.79%	874 K	521 K
TreeLogicNet-M	71.38%	7.00 M	3.66 M
Ours-S	65.85%	291 K	174 K
Ours-M	69.44%	582 K	389 K
Ours-L	72.09%	2.33 M	1.09 M

ceptive field. TreeLogicNet restricts every kernel to see two neighboring channels, while we further restrict the number of channels seen by each kernel to one. We will show that such restriction improves performance significantly, and hypothesize that it is due to the destructive effect of thermometer encoding on natural images.

Main Results The results on MNIST and CIFAR-10 are summarized in Table 3 and Table 4, respectively. Our architecture consistently outperforms TreeLogicNet with fewer neurons. On MNIST, our medium model outperforms the large TreeLogicNet with 22x fewer (520K vs 11.8M) neurons. On CIFAR-10, our large model achieves 0.71% higher accuracy (72.09% vs 71.38%) with 3x fewer (2.33M vs 7M) neurons than TreeLogicNet. We remark that larger models reported in Petersen et al. (2024) are not Boolean networks since they contain floating-point feature extraction layers, and are thus excluded in the comparison.

The Paradox of Channel Restriction We conduct an extensive study on the effect of limiting the number of channels seen by each convolutional kernel here. Fig. 7 shows the effect of limiting the number of channels accessible to each kernel on CIFAR-10 with our medium model. We find a similar conclusion as in Petersen et al. (2024): limiting the number of accessible channels improves performance significantly. In particular, restricting each kernel to see only one channel achieves the best accuracy, 4.56% higher than seeing all channels (69.46% vs 64.90%). This phenomenon leads to a direct paradox: restricting the visible channels to one means that composition of convolutional layers can no longer mix information across channels. Intuitively, this should have hurt the performance instead. We hypothesize that this is due to the destructive effect of thermometer encoding on natural images. As visualized

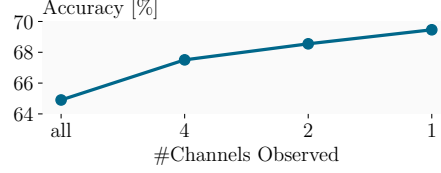


Figure 7. The effect of limiting the number of channels seen by each convolutional kernel on CIFAR-10. Note that the x-axis is unequally spaced.

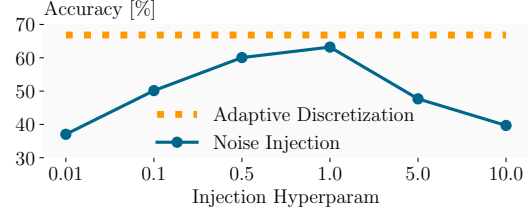


Figure 8. Comparison between noise injection and the proposed adaptive discretization. Note that the x-axis is unequally spaced.

in §A, thermometer encoding breaks the complementary information across channels in natural images, sometimes even completely removing the information in some channels. This might lead to interference across channels when multiple channels are seen by the same kernel. Therefore, a better input encoding scheme that preserves cross-channel information might allow efficient information composition across channels and further improve the performance of convolutional Boolean networks. We leave further exploration of this paradox to future work.

5.3. Adaptive Discretization

In this part, we evaluate the proposed adaptive discretization strategy, comparing it against Gumbel noise injection. In addition to test accuracy, we also measure the discretization gap, defined as the accuracy difference between the relaxed model before discretization and the discretized Boolean network after discretization, following Yousefi et al. (2025).

Main Results Fig. 8 compares the proposed adaptive discretization against Gumbel noise injection on CIFAR-10 with our medium convolutional model. We sweep the hyperparameter for Gumbel noise injection for a fair comparison. As shown in Fig. 8, our method consistently outperforms Gumbel noise injection in test accuracy. Further, the adaptive discretization significantly reduces the training cost, since discretized layers are more efficient in both forward and backward passes. For example, after discretizing four convolutional layers, the model trains 1.8x faster than the original model. In contrast, Gumbel noise injection leads to computational overhead throughout training.

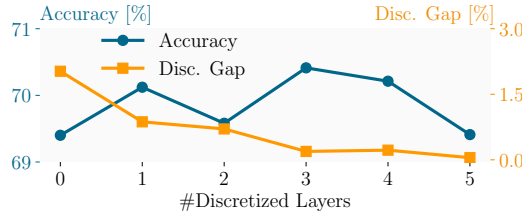


Figure 9. The effect of the number of discretized layers during training on the accuracy and discretization gap.

Adaption Reduces Discretization Gap Progressively

We conduct an ablation study on CIFAR-10 with our medium convolutional model, varying the number of layers discretized during training from 1 to 5 (the model has 6 layers in total). As shown in Fig. 9, progressively discretizing more layers during training consistently reduces the discretization gap, demonstrating the effectiveness of the proposed adaptive discretization strategy. However, due to the limited number of training steps, progressively discretizing all layers during training does not lead to the best accuracy after discretization, as the model has insufficient resource to learn better solutions. In practice, we find that progressively discretizing all convolutional layers works well for all models, achieving a good balance between reducing the discretization gap and allowing sufficient learning. This is possibly because non-convolutional layers can converge steadily without discretization during training (c.f. Fig. 4). Therefore, for our final models, we always adaptively discretize all convolutional layers, as described in §4.3.

5.4. Combined Results

We combine all proposed methods together and evaluate the final performance on MNIST and CIFAR-10. The results are summarized in Table 5. On MNIST, our small and medium models achieve 99.35% and 99.41% accuracy, outperforming the large TreeLogicNet with 45x and 22x fewer neurons (260K and 520K vs 11.8M), respectively. After pruning, our models demonstrate a reduction in #BOPs by 37x and 27x (168K and 228K vs 6.2M), respectively. On CIFAR-10, our large model achieves 72.67% accuracy, outperforming TreeLogicNet with 3x fewer neurons and #BOPs. We further report the performance variance over random seeds in §B. These results validate the effectiveness and stability of the proposed methods in learning compact and accurate Boolean networks.

6. Discussion

Despite the promising results, several limitations are open for future work. First, while our method effectively reduces the number of neurons during training and the number of Boolean operations at inference, the training process still relies on floating-point computations, which can be resource-intensive for large models since each neuron con-

Table 5. The comparison between our final models and the state-of-the-art TreeLogicNet.

Dataset	Method	Acc.	#neurons	#BOPs
MNIST	TreeLogicNet-S	97.81%	185 K	117 K
	TreeLogicNet-M	98.95%	740 K	427 K
	TreeLogicNet-L	99.32%	11.8 M	6.20 M
	Ours-S	99.35%	260 K	168 K
CIFAR-10	Ours-M	99.41%	520 K	228 K
	TreeLogicNet-S	59.79%	874 K	521 K
	TreeLogicNet-M	71.38%	7.00 M	3.66 M
	Ours-T	62.34%	145 K	100 K
	Ours-S	66.92%	291 K	197 K
	Ours-M	70.21%	582 K	337 K
	Ours-L	72.67%	2.33 M	1.08 M

tributes 16 floating-point weights. Second, our current experiments focus on vision benchmarks; extending the evaluation to other modalities such as texts and sequences will provide a further understanding of the capability of compact Boolean networks. Third, our method does not take into account the advanced logic synthesis techniques for network optimization; further exploiting certain properties of such methods to train synthesis-friendly networks might lead to even more compact models after synthesis. Finally, this work only considers the training process of the Boolean network; the design of input encoding and output decoding schemes deserves further investigation.

7. Conclusion

This work addresses learning compact Boolean networks by tackling three key challenges: efficient connection learning, compact convolutional architecture, and discretization-aware training. We propose a novel parameterization for Boolean neurons that allows aggregating information from multiple connections, along with an adaptive resampling strategy that continuously explores new connections, to enable efficient connection learning without additional parameters. Additionally, we redesign the convolutional Boolean architecture, demonstrating significant reductions in Boolean operations with improved performance compared to prior designs. Finally, we introduce an adaptive discretization strategy that progressively adapt the network to the discretization process during training, effectively reducing the accuracy drop after discretization. Extensive empirical results on standard vision benchmarks validate the effectiveness of our proposed methods, achieving better accuracy with up to 37x fewer Boolean operations compared to prior state-of-the-art methods.

Impact Statement

This paper presents work whose goal is to advance the field of Machine Learning. There are many potential societal consequences of our work, none which we feel must be specifically highlighted here.

References

Andronic, M. and Constantinides, G. A. Neuralut-assemble: Hardware-aware assembling of sub-neural networks for efficient lut inference. In *2025 IEEE 33rd Annual International Symposium on Field-Programmable Custom Computing Machines (FCCM)*. IEEE, 2025. doi: 10.1109/FCCM62733.2025.00077.

Arora, S. and Barak, B. *Computational complexity: a modern approach*. Cambridge University Press, 2009.

Bacellar, A. T., Susskind, Z., Breternitz Jr, M., John, E., John, L. K., Lima, P., and França, F. M. Differentiable weightless neural networks. *arXiv preprint arXiv:2410.11112*, 2024.

Bjesse, P. and Boralv, A. DAG-aware circuit compression for formal verification. In *IEEE/ACM International Conference on Computer Aided Design, 2004. ICCAD-2004.*, pp. 42–49, November 2004.

Brayton, R. and Mishchenko, A. ABC: An academic industrial-strength verification tool. In *Computer Aided Verification (CAV)*, volume 6174 of *Lecture Notes in Computer Science*, pp. 24–40. Springer, 2010. doi: 10.1007/978-3-642-14295-6_5.

Bührer, S., Plesner, A., Aczel, T., and Wattenhofer, R. Recurrent deep differentiable logic gate networks. In *Proceedings of the 2nd International Workshop on Edge and Mobile Foundation Models*, pp. 31–36, 2025.

Cassidy, O., Andronic, M., Coward, S., and Constantinides, G. A. Reducedlut: Table decomposition with “don’t care” conditions. In *Proceedings of the 2025 ACM/SIGDA International Symposium on Field-Programmable Gate Arrays (FPGA ’25)*, pp. 36–42. ACM, 2025. doi: 10.1145/3706628.3708823.

Cheng, H., Zhang, M., and Shi, J. Q. A survey on deep neural network pruning: Taxonomy, comparison, analysis, and recommendations. *IEEE Transactions on Pattern Analysis and Machine Intelligence*, 2024.

Florio, M. and Martins, R. Sat-based learning of compact binary decision diagrams for classification. *Proceedings of the International Conference on Principles and Practice of Constraint Programming (CP)*, 2023.

Fojcik, K., Zioma, R., and Armaitis, J. Lilogic net: Compact logic gate networks with learnable connectivity for efficient hardware deployment. *arXiv preprint arXiv:2511.12340*, 2025.

Frankle, J. and Carbin, M. The lottery ticket hypothesis: Finding sparse, trainable neural networks. In *International Conference on Learning Representations*, 2019.

Ganai, M. K. and Kuehlmann, A. *On-the-fly compression of logical circuits*. IBM Thomas J. Watson Research Division, 2000.

Gholami, A., Kim, S., Dong, Z., Yao, Z., Mahoney, M. W., and Keutzer, K. A survey of quantization methods for efficient neural network inference. *CoRR*, abs/2103.13630, 2021. URL <https://arxiv.org/abs/2103.13630>.

Kim, Y. Deep stochastic logic gate networks. *IEEE Access*, 11:122488–122501, 2023.

Kingma, D. P. and Ba, J. Adam: A method for stochastic optimization. *International Conference on Learning Representations (ICLR)*, 2015.

Korinek, L. convlogic: Community implementation of convolutional logic networks. <https://github.com/lkorinek/convlogic>, 2025. GitHub repository, accessed 2026-01-26.

Krizhevsky, A., Hinton, G., et al. Learning multiple layers of features from tiny images. Technical report, University of Toronto, 2009.

LeCun, Y., Bottou, L., Bengio, Y., and Haffner, P. Gradient-based learning applied to document recognition. *Proceedings of the IEEE*, 86(11):2278–2324, 1998.

Li, Y., Liu, M., Ren, M., Mishchenko, A., and Yu, C. DAG-aware synthesis orchestration. *IEEE Transactions on Computer-Aided Design of Integrated Circuits and Systems (TCAD)*, 2024. doi: 10.1109/TCAD.2024.3397052.

Liu, K., Zheng, Q., Tao, K., Li, Z., Qin, H., Li, W., Guo, Y., Liu, X., Kong, L., Chen, G., et al. Low-bit model quantization for deep neural networks: A survey. *arXiv preprint arXiv:2505.05530*, 2025.

Micheli, G. D. *Synthesis and optimization of digital circuits*. McGraw-Hill Higher Education, 1994.

Mishchenko, A., Chatterjee, S., and Brayton, R. DAG-aware AIG rewriting a fresh look at combinational logic synthesis. In *Proceedings of the 43rd Annual Conference on Design Automation - DAC ’06*, pp. 532, San Francisco, CA, USA, 2006a. ACM Press. doi: 10.1145/1146909.1147048.

Mishchenko, A., Chatterjee, S., and Brayton, R. K. Dag-aware AIG rewriting: A fresh look at combinational logic synthesis. In *Proceedings of the 43rd ACM/IEEE Design Automation Conference (DAC)*, pp. 532–536, 2006b. doi: 10.1145/1146909.1147048.

Petersen, F., Borgelt, C., Kuehne, H., and Deussen, O. Deep differentiable logic gate networks. *Advances in Neural Information Processing Systems*, 35:2006–2018, 2022.

Petersen, F., Kuehne, H., Borgelt, C., Welzel, J., and Ermon, S. Convolutional differentiable logic gate networks. *Advances in Neural Information Processing Systems*, 37:121185–121203, 2024.

Qiu, J. et al. End-to-end learning of ordered binary decision diagrams. In *Proceedings of the ACM International Conference on Information and Knowledge Management (CIKM)*, 2025.

Riener, H., Haaswijk, W., Mishchenko, A., Micheli, G. D., and Soeken, M. On-the-fly and DAG-aware: Rewriting boolean networks with exact synthesis. In *Design, Automation & Test in Europe Conference & Exhibition (DATE)*, 2019. doi: 10.23919/DATE.2019.8715185.

Riener, H., Lee, S.-Y., Mishchenko, A., and De Micheli, G. Boolean Rewriting Strikes Back: Reconvergence-Driven Windowing Meets Resynthesis. In *2022 27th Asia and South Pacific Design Automation Conference (ASP-DAC)*, pp. 395–402, Taipei, Taiwan, January 2022. IEEE. doi: 10.1109/ASP-DAC52403.2022.9712526.

Rudell, R. and Sangiovanni-Vincentelli, A. Multiple-Valued Minimization for PLA Optimization. *IEEE Transactions on Computer-Aided Design of Integrated Circuits and Systems*, 6(5):727–750, September 1987. ISSN 1937-4151. doi: 10.1109/TCAD.1987.1270318.

Rüttgers, L., Aczel, T., Plesner, A., and Wattenhofer, R. Light differentiable logic gate networks. *arXiv preprint arXiv:2510.03250*, 2025.

Shati, P., Cohen, E., and McIlraith, S. A. Sat-based learning of compact binary decision diagrams for classification. In Yap, R. H. C. (ed.), *29th International Conference on Principles and Practice of Constraint Programming (CP 2023)*, volume 280 of *Leibniz International Proceedings in Informatics (LIPIcs)*, pp. 33:1–33:19. Schloss Dagstuhl – Leibniz-Zentrum für Informatik, 2023. doi: 10.4230/LIPIcs.CP.2023.33.

Umuroglu, Y., Akhauri, Y., Fraser, N. J., and Blott, M. High-throughput dnn inference with logicnets. In *2020 IEEE 28th Annual International Symposium on Field-Programmable Custom Computing Machines (FCCM)*. IEEE, 2020. doi: 10.1109/FCCM48280.2020.00071.

Wang, E., Davis, J. J., Cheung, P. Y. K., and Constantinides, G. A. Lutnet: Rethinking inference in fpga soft logic. In *2019 IEEE 27th Annual International Symposium on Field-Programmable Custom Computing Machines (FCCM)*, pp. 26–34. IEEE, 2019. doi: 10.1109/FCCM.2019.00014.

Weng, O., Andronic, M., Zuberi, D., Chen, J., Geniesse, C., Constantinides, G., Tran, N., Fraser, N., Duarte, J., and Kastner, R. Greater than the sum of its lut: Scaling up lut-based neural networks with amigolut. In *Proceedings of the 2025 ACM/SIGDA International Symposium on Field-Programmable Gate Arrays (FPGA '25)*, pp. 25–35. ACM, 2025. doi: 10.1145/3706628.3708874.

Yousefi, S., Plesner, A., Aczel, T., and Wattenhofer, R. Mind the gap: Removing the discretization gap in differentiable logic gate networks. *arXiv preprint arXiv:2506.07500*, 2025.

Zantedeschi, V., Kusner, M. J., and Niculae, V. Learning binary decision trees by argmin differentiation. In *Proceedings of the 38th International Conference on Machine Learning*, volume 139 of *Proceedings of Machine Learning Research*, pp. 12298–12309. PMLR, 2021. URL <https://proceedings.mlr.press/v139/zantedeschi21a.html>.

A. Visualization of Thermometer Encoding Effects

As shown in Fig. 10, the thermometer-encoded channels lose most color information and only retain partial edge information. Further, only a small portion of channels contain non-trivial and non-overlapping information; in most cases, merely a single channel retains label information, up to repetition. This phenomenon inspires our hypothesis in §5.2.



Figure 10. Illustration of the destructive effect of thermometer encoding on the channels of natural images from CIFAR-10.

B. Variance Across Random Seeds

To verify the stability of our methods, we repeat the main results in §5.1 and §5.2 with different random seeds and report the mean and standard deviation in Table 6, Table 7, Table 8, and Table 9, respectively. Results show that our method consistently outperforms the baselines with a clear margin under different random seeds, demonstrating the robustness of our approach.

Table 6. Statistics on MNIST for connection learning.

Method	Acc.	#neurons	#BOPs
DiffLogicNet (small)	$97.03\% \pm 0.10\%$	48.0 K	27.0 ± 0.1 K
DiffLogicNet (medium)	$98.78\% \pm 0.02\%$	384 K	215 ± 1 K
Ours (small)	$97.77\% \pm 0.13\%$	48.0 K	25.2 ± 0.4 K
Ours (medium)	$99.06\% \pm 0.03\%$	384 K	190 ± 1 K

Table 7. Statistics on CIFAR-10 for connection learning.

Method	Acc.	#neurons	#BOPs
DiffLogicNet (small)	$52.70\% \pm 0.15\%$	48.0 K	27.0 ± 0.7 K
DiffLogicNet (medium)	$59.74\% \pm 0.11\%$	512 K	311 ± 1 K
DiffLogicNet (large)	$61.48\% \pm 0.76\%$	1.28 M	780 ± 2 K
Ours (small)	$55.81\% \pm 0.33\%$	48.0 K	27.6 ± 0.3 K
Ours (medium)	$62.46\% \pm 0.27\%$	512 K	296 ± 2 K
Ours (large)	$64.16\% \pm 0.26\%$	1.28 M	655 ± 1 K

Table 8. Statistics on MNIST for convolution.

Method	Acc.	#neurons	#BOPs
TreeLogicNet-S	$97.76\% \pm 0.04\%$	220 K	120 ± 1 K
TreeLogicNet-M	$98.87\% \pm 0.12\%$	883 K	433 ± 2 K
TreeLogicNet-L	$99.28\% \pm 0.03\%$	11.8 M	6.20 ± 0.03 M
Ours-S	$99.33\% \pm 0.01\%$	260 K	168 ± 2 K
Ours-M	$99.34\% \pm 0.07\%$	520 K	259 ± 3 K

Table 9. Statistics on CIFAR-10 for convolution.

Method	Acc.	#neurons	#BOPs
TreeLogicNet-S	$59.47\% \pm 0.35\%$	874 K	538 ± 8 K
TreeLogicNet-M	$71.30\% \pm 0.06\%$	7.00 M	3.76 ± 0.06 M
Ours-T	$62.24\% \pm 0.07\%$	145 K	100 ± 1 K
Ours-S	$66.74\% \pm 0.18\%$	291 K	191 ± 12 K
Ours-M	$69.90\% \pm 0.24\%$	582 K	374 ± 26 K
Ours-L	$72.33\% \pm 0.23\%$	2.33 M	1.08 ± 0.12 M

C. Implementation for TreeLogicNet

Since Petersen et al. (2024) did not release the official implementation of TreeLogicNet, we use a community implemented version available at Korinek (2025). To verify the correctness of this implementation, we compare the test accuracies obtained from the GitHub implementation and those reported in Petersen et al. (2024). The results are summarized in

Table 10. A comparison between the reported accuracy from Petersen et al. (2024) and the community implemented TreeLogicNet (named ConvLogic).

Model	Petersen et al. (2024) reported	ConvLogic reported	ConvLogic + aug
TreeLogicNet-S	60.38%	59.84%	59.79%
TreeLogicNet-M	71.01%	69.15%	71.38%

Table 10. While the reported accuracies from the community implementation are slightly lower than those reported in Petersen et al. (2024), we find that simply applying the same data augmentation strategy as in our experiments during training closes the performance gap. This partially confirms the correctness of the community implementation, allowing us to use it as a baseline for convolutional Boolean networks in our experiments.

D. Bivariate Boolean Functions

We include the truth table of all sixteen bivariate Boolean functions in Table 11. For example, B_1 is the constant 0 function, B_2 is the AND function, B_4 is the identity function, B_8 is the OR function, and B_{16} is the constant 1 function.

Table 11. The truth table of sixteen bivariate Boolean functions.

x_1	x_2	B_1	B_2	B_3	B_4	B_5	B_6	B_7	B_8	B_9	B_{10}	B_{11}	B_{12}	B_{13}	B_{14}	B_{15}	B_{16}
0	0	0	0	0	0	0	0	0	0	1	1	1	1	1	1	1	1
0	1	0	0	0	0	1	1	1	1	0	0	0	0	1	1	1	1
1	0	0	0	1	1	0	0	1	1	0	0	1	1	0	0	1	1
1	1	0	1	0	1	0	1	0	1	0	1	0	1	0	1	0	1

E. Pruning Algorithm

We present the pruning algorithm used to compute the effective number of Boolean operations (#BOPs) after training here. This pruning algorithm serves as a minimal post-processing step to remove trivial and disconnected neurons from the learned network, providing a more accurate estimate of the inference complexity. In addition, it provides insights into the potential of further applying logic synthesis techniques to optimize the learned networks.

First, we exclude constant neurons (i.e., B_1 and B_{16} , since we can implement all of them with a single constant neuron in the circuit), identity neurons (i.e., B_4 and B_6 , since they can be directly removed from the circuit) and negation neurons (i.e., B_{11} and B_{13} , since they can be composed with the preceding or following neurons). Then, we remove all neurons that are not connected to the final output layer and therefore can be safely eliminated without affecting the network’s output. A detailed pruning procedure is provided in Algorithm 3. We remark that since only #BOPs are desired, we used an alternative GPU-based implementation to speed up the computation.

When comparing against DiffLogicNet and TreeLogicNet, we apply the same pruning procedure to their learned networks to ensure a fair comparison of #BOPs. Therefore, this pruning step is weaker than the logic synthesis techniques used in Petersen et al. (2022; 2024). Nevertheless, we find the #BOPs after pruning is comparable to those reported in Petersen et al. (2022; 2024), indicating that our pruning procedure is sufficient for estimating the inference complexity of Boolean networks.

F. Further Experimental Details

Model Architectures We list the detailed configurations of our convolutional architecture used in the experiments below. The variants T (tiny), S (small), M (medium), and L (large) correspond to $k = 64, 128, 256$, and 1024 , respectively. N denotes the number of thresholds used in the thermometer encoding of the input image. For MNIST, we set $N = 1$; for CIFAR-10, we set $N = 3$ for tiny and small models, $N = 7$ for medium models, and $N = 31$ for large models.

Algorithm 3 Pruning

```

Input: trained Boolean network
Output: pruned Boolean network, #BOPs after pruning
pruned  $\leftarrow$  output neurons  $\cup \{0, 1\}$ , BOPs  $\leftarrow 0$ 
Q  $\leftarrow$  queue(output neurons)
repeat
    current  $\leftarrow$  Q.dequeue()
    if current is constant then
        connect to the constant neuron in the pruned network instead
    else if current is identity or negation then
         $n \leftarrow$  the nontrivial input neuron of current
        add  $n$  to pruned and Q, respectively, if  $n$  is not already in pruned
        if current is negation then
            adjust the connection from  $n$  to the neurons accepting current as their input to account for the negation
        end if
    else
        BOPs  $\leftarrow$  BOPs + 1
         $n_1, n_2 \leftarrow$  two input neurons of current
        add  $n_1, n_2$  to pruned and Q, respectively, if they are not already in pruned
    end if
until Q is empty

```

MNIST Model Architecture:

- **Layer 1:** Convolutional layer with kernel size 3×3 , stride 2, and padding 1, mapping $(N, 28, 28) \rightarrow (k, 14, 14)$.
- **Layer 2:** Convolutional layer with kernel size 3×3 , stride 1, and padding 1, mapping $(k, 14, 14) \rightarrow (k, 14, 14)$.
- **Layer 3:** Convolutional layer with kernel size 3×3 , stride 2, and padding 1, mapping $(k, 14, 14) \rightarrow (4k, 7, 7)$.
- **Layer 4:** Convolutional layer with kernel size 3×3 , stride 1, and padding 1, mapping $(4k, 7, 7) \rightarrow (4k, 7, 7)$.
- **Layer 5:** Flatten operation.
- **Layer 6:** Logic layer mapping $196k \rightarrow 625k$ neurons.
- **Layer 7:** Logic layer mapping $625k \rightarrow 625k$ neurons.
- **Layer 8:** Group-sum (population count) layer with 10 output groups.

CIFAR-10 Model Architecture:

- **Layer 1:** Convolutional layer with kernel size 3×3 , stride 2, and padding 1, mapping $(3N, 32, 32) \rightarrow (k, 16, 16)$.
- **Layer 2:** Convolutional layer with kernel size 3×3 , stride 1, and padding 1, mapping $(k, 16, 16) \rightarrow (k, 16, 16)$.
- **Layer 3:** Convolutional layer with kernel size 3×3 , stride 2, and padding 1, mapping $(k, 16, 16) \rightarrow (4k, 8, 8)$.
- **Layer 4:** Convolutional layer with kernel size 3×3 , stride 1, and padding 1, mapping $(4k, 8, 8) \rightarrow (4k, 8, 8)$.
- **Layer 5:** Flatten operation.
- **Layer 6:** Logic layer mapping $256k \rightarrow 625k$ neurons.
- **Layer 7:** Logic layer mapping $625k \rightarrow 625k$ neurons.
- **Layer 8:** Group-sum (population count) layer with 10 output groups.

Table 12. The comparison between Gaussian and residual initialization on regular models trained with our proposed method.

Dataset	Model	Gaussian	Residual
MNIST	small	97.95%	97.89%
	medium	99.10%	98.61%
CIFAR-10	small	56.13%	56.09%
	medium	62.84%	63.52%
	large	64.53%	65.42%

Training Details We initialize the weights of regular models using a Gaussian distribution $\mathcal{N}(0, 1)$ to enable fair comparison with DiffLogicNet, while for convolutional models we adopt the residual initialization as in TreeLogicNet, which set the normalized weight of B_4 to 0.9 and the normalized weight of others to $\frac{0.1}{15}$. We further compare Gaussian and residual initialization for regular models on MNIST and CIFAR-10. As shown in Table 12, residual initialization does not consistently outperform Gaussian initialization on regular models; nevertheless, when the task becomes challenging (CIFAR-10) and the model grows large (M and L), residual initialization shows improved performance.

All models are trained using the Adam optimizer (Kingma & Ba, 2015). We use a constant learning rate of 0.01 for regular models and 0.02 for convolutional models, with a batch size of 128 throughout. We remark that further use learning rate scheduling does not improve performance, potentially because the improved minimum in the relaxed form does not reflect improvements on the discretized model. Regular models are trained for 300K steps and evaluated every 1K steps to select the best checkpoint. Tiny, small and medium convolutional models are trained for 600K steps and evaluated every 2K steps, while the large convolutional model is trained for 700K steps and evaluated at the same frequency. We find weight decay to be unhelpful in our experiments and thus do not apply it.

We initialize the parameterization of the connection learning as follows. At initialization, $\mathbf{k} = [1, \dots, 16]$, i.e., every neuron has 16 distinct Boolean operations (c.f., §D). For convolutional layers, we sample (\mathbf{p}, \mathbf{q}) from the receptive field (3x3) uniformly at random with replacement. For non-convolutional layers, since the possible input neuron set is large, we initialize (\mathbf{p}, \mathbf{q}) in the following way to ensure information coverage. Let d_{in} and d_{out} denote the input and output dimensions of the layer, respectively. We assume $2 \times d_{\text{out}} \geq d_{\text{in}}$, otherwise some input neurons cannot be considered by the final network. Given this, let $r := \lfloor 2 \times d_{\text{out}} / d_{\text{in}} \rfloor$, we assign all input neurons to the first $r \times d_{\text{in}}$ input slots (with r times of repetition) and sample the remaining slots from all input neurons uniformly at random with replacement; afterwards, we shuffle the input slots to ensure randomness. This process is independently repeated for 16 times to initialize each entry of (\mathbf{p}, \mathbf{q}) . When resampling is activated, we resample the corresponding $(\mathbf{p}_i, \mathbf{q}_i)$ uniformly at random, in the receptive field for convolutional layers and from all input neurons for non-convolutional layers. \mathbf{k}_i are sampled uniformly from $\{1, \dots, 16\}$ during resampling.

The large convolutional model, when trained with a single GeForce RTX 5090 GPU, has a peak memory usage of 6.1 GB and a throughput of 9.2 steps per second.

Hyperparameters We list detailed hyperparameter settings in Table 13. The original hyperparameter is adopted for DiffLogicNet and TreeLogicNet.

For resampling, we employ an exponential moving average (EMA) with momentum $\rho = 0.99$ and a stability threshold $\epsilon = 5 \times 10^{-4}$ across all experiments. The resampling patience T is tuned based on the size of the model; larger models have larger T . Adaptive discretization is applied only to convolutional models, using the same EMA momentum $\rho = 0.99$, stability threshold $\epsilon = 5 \times 10^{-4}$, and a fixed patience $T = 200$.

For tiny, small and medium convolutional models, resampling is enabled during the first 400 K training steps, then it is disabled and adaptive discretization is activated. For the large convolutional model, resampling is performed for 500 K steps, followed by adaptive discretization for the remainder of training (200 K steps).

Table 13. Hyperparameter settings for regular and convolutional models.

Structure	Model	Dataset	Group Sum	Temp. τ	Patience T
Regular	Ours (small)	MNIST	10	100	
	Ours (medium)	MNIST	45	1000	
	Ours (small)	CIFAR-10	33	100	
	Ours (medium)	CIFAR-10	100	500	
	Ours (large)	CIFAR-10	100	1000	
	Ours-S	MNIST	40	100	
Convolutional	Ours-M	MNIST	63	100	
	Ours-T	CIFAR-10	20	100	
	Ours-S	CIFAR-10	40	100	
	Ours-M	CIFAR-10	63	100	
	Ours-L	CIFAR-10	160	15000	